ISSN: 1410-8917
Jurnal Kimia Sains & Aplikasi
e-ISSN: 2597-9914

Jurnal Kimia Sains dan Aplikasi 27 (5) (2024): 226-231

Jurnal Kimia Sains dan Aplikasi
Journal of Scientific and Applied Chemistry

Journal homepage: http://ejournal.undip.ac.id/index.php/ksa

The Effect of Calcination Temperature on the Characteristics of CeO_2 Synthesized Using the Precipitation Method

Zidan Alfian Bahtiar [1], Tri Windarti [1,*], Dwi Hudiyanti [1]

[1] Chemistry Department, Faculty of Sciences and Mathematics, Diponegoro University, Jl. Prof. Soedarto, SH., Tembalang, Semarang, Indonesia

* Corresponding author: tri.windarti@lecturer.undip.ac.id

https://doi.org/10.14710/jksa.27.5.226-231

Article Info

Article history:

Received: 18th January 2024
Revised: 22nd April 2024
Accepted: 26th April 2024
Online: 31st May 2024

Keywords:
Cerium oxide; Calcination; Precipitation

Abstract

Cerium oxide (CeO_2) was synthesized using the precipitation method at various calcination temperatures ranging from 500 to 700°C. Cerium(III) nitrate hexahydrate ($Ce(NO)_3.6H_2O$) was used as the precursor for cerium, while Cetyltrimethylammonium bromide (CTAB) acted as the morphology-directing agent. Characterization results indicated that pure CeO_2 was obtained at all calcination temperature variations. Calcination temperature influences crystallinity, crystal size, and CeO_2 crystal parameters. The crystallinity and crystal size of CeO_2 increased with the rising calcination temperature, reaching values of 81.1–84.5% and 15.58–23.12 nm, respectively, along with larger crystal parameters as the temperature increased (a = 5.406–5.410 Å). Surface morphology showed irregular shapes of CeO_2 particles, with decreasing sizes as the calcination temperature increased, ranging from 0.2-5.6 µm at 600°C to 0.12-2.9 µm at 700°C. The Ce/O ratio on the surface increased with the rising calcination temperature, reaching a range of 0.48–0.57. CeO_2 obtained from calcination at 600°C exhibited the highest fluorescence emission intensity (λ= 496 nm), indicating the least oxygen vacancies presence. Therefore, for antioxidant and catalyst applications, it is preferable to calcinate CeO_2 at 700°C.

1. Introduction

Cerium oxide (CeO_2) is a metal oxide that has a fluorite cubic structure (FCC) [1]. With a redox potential of 1.7 V, it possesses the unique property of being able to undergo redox cycling between $Ce^{3+} \rightleftharpoons Ce^{4+}$ [2, 3]. The redox cycle allows CeO_2 to be applied as an energy storage device [4], materials for making supercapacitors [5], catalysts [6], nanozymes in plants [7], and antioxidants [8, 9]. As antioxidants, CeO_2 are capable of degrading ·OH radicals, with their activity being influenced by several factors such as particle size and the presence of crystal defects [10].

The synthesis of CeO_2 can be carried out using several methods, such as reverse microemulsion [6], hydrothermal [11], sol-gel [12, 13, 14], green synthesis [15, 16, 17] combustion [18, 19], ball-milling [20, 21], precipitation and coprecipitation [22, 23, 24, 25]. The precipitation method is the most commonly used because it is easy to perform, cost-effective, has high reaction rates, and can be conducted on both large and small scales. Synthesis of CeO_2 using the precipitation method can be carried out by adding a solution of cerium (III) nitrate to a base solution, such as ammonium hydroxide, to form a precipitate. The precipitate is then dried and calcined at temperatures ranging from 300-700°C [26].

The characteristics of CeO_2 produced, such as particle shape and size, crystalline properties, and morphology, are influenced by the temperature and duration of calcination [26]. The characteristics of CeO_2 significantly impact its performance when used as an antioxidant [27]. Literature studies indicate that the crystallite and particle size tend to increase with the rise in calcination temperature from 350 to 700°C, while the surface area tends to decrease. The best radioprotective and antioxidant activities occur at a calcination temperature of 500°C [22, 26, 27, 28].

The synthesis of inorganic materials by the precipitation method typically results in particles with non-uniform shapes and sizes. Surfactants can be introduced to address this issue, as they are capable of forming micelles that regulate particle growth, resulting in particles with uniform shapes and sizes [29]. Cetyltrimethylammonium bromide (CTAB) surfactant has been proven to reduce particle size in the synthesis of CeO_2 using the coprecipitation method [30].

This study aims to synthesize CeO_2 using the precipitation method, with cerium (III) nitrate hexahydrate serving as the cerium precursor and CTAB surfactant acting as the morphology-directing agent. Based on literature studies, it can be hypothesized that varying the temperature will affect the morphology of CeO_2. Therefore, this study varies calcination temperatures at 500°C, 600°C, and 700°C to examine its impact on the characteristics of CeO_2, including product purity, crystallinity, particle size and shape, and fluorescence properties.

2. Experimental

2.1. Materials

The materials used in this study were cerium (III) nitrate hexahydrate (Merck), cetyltrimethylammonium bromide (CTAB) (Sigma Aldrich), 32% NH_4OH (Merck), and distilled water.

2.2. Equipment

The equipment used in this study included a furnace, magnetic stirrer, FTIR (Thermo Scientific Nicolet iS10), XRD (BRUKER AXS D8), SEM-EDS (JSM-6510LA), and fluorescence spectrophotometer (Cary Eclipse Fluorescence Spectrophotometer).

2.3. Method

A 50 mL cerium precursor solution was produced by dissolving 21.71 grams of cerium (III) nitrate hexahydrate and 0.0164 grams of CTAB in distilled water. Subsequently, the solution was treated with 32% NH_4OH until a precipitate formed or the solution reached a pH of 9. Afterward, the solution was allowed to stand for 48 hours, and the precipitate was separated from the solution. The precipitate was then dried in an oven at 60°C for three hours and subsequently subjected to calcination at varying temperatures of 500, 600, and 700°C for 2 hours each. The resulting samples were respectively labeled Ce500, Ce600, and Ce700.

2.4. Characterization

Functional group analysis was performed using FTIR with the KBr pellet method within the wavenumber range of 500-4000 cm^{-1}. Crystallinity and crystal size were assessed utilizing XRD with a 2θ angle range of 25-100°. Surface morphology profiles were acquired through imaging with SEM-EDS. The effect of temperature on the fluorescence properties of the resulting CeO_2 was investigated using a fluorescence spectrophotometer at a wavelength range of 200-600 nm.

3. Results and Discussion

Figure 1 shows the physical appearance of the CeO_2 powder produced at different calcination temperatures. CeO_2 has a pale yellow powder form at all calcination temperatures with a weight of about 2.7 grams or a yield of about 93%. The formation of CeO_2 is believed to follow Reaction (1).

$$Ce(NO_3)_3.6H_2O \rightarrow Ce^{3+} + 3NO_3^{-1} + 6H_2O \quad (1)$$

The addition of ammonia solution (NH_4OH) as an OH^- source in the solution will lead to precipitation according to Reaction (2).

$$Ce^{3+} + 3OH^- \rightarrow Ce(OH)_3 \quad (2)$$

In a high pH environment, $Ce(OH)_3$ can be oxidized to $Ce(OH)_4$, and after calcination, CeO_2 can be formed (Reaction 3) [31, 32, 33].

$$Ce(OH)_3 + ½O_2 \rightarrow Ce(OH)_4 \quad (3)$$

The FTIR spectra of synthesized CeO_2 (Figure 2) show similarities with the FTIR spectra of CeO_2 in the study conducted by Jayakumar *et al.* [34]. The peak around the wavenumber 850 cm^{-1} indicates Ce-O vibrations. The broad peak around 3600-3400 cm^{-1} represents O-H vibrations from trapped water molecules, evidenced by the peak at 1625 cm^{-1} [29, 30, 31]. The peaks around 1320 cm^{-1} and 1060 cm^{-1} are vibrations from "carbonate-like" species formed due to the interaction between CO_2 and CO on the surface of CeO_2 [34, 35]. The transmittance of the O-H vibration peak in the Ce700 sample is smaller than in the Ce500 and Ce600 samples. This phenomenon is consistent with the research results of Sheena *et al.* [36], which indicate that the intensity of the O-H vibrations decreases with increasing calcination temperature.

Figure 1. Synthesized CeO_2: (A) Ce500, (B) Ce600, and (C) Ce700

Table 1. Analysis results based on XRD data of CeO_2 samples

hkl	2θ(°)			Relative intensity (%)			FWHM		
	Ce500	Ce600	Ce700	Ce500	Ce600	Ce700	Ce500	Ce600	Ce700
111	28.56	28.56	28.54	100	100	100	0.54	0.46	0.37
200	33.09	33.10	33.07	32.2	31	31.3	0.51	0.42	0.37
320	47.51	47.52	47.49	78.6	79.3	97	0.67	0.56	0.41
311	56.37	56.38	56.35	71.6	69.7	88.5	0.68	0.66	0.46

Table 2. Analysis results based on XRD data of CeO_2 samples

Sample	Crystallinity (%)	Lattice parameter (Å)	Crystallite size (nm)
Ce500	81.1	5.406	15.58
Ce600	82.8	5.406	18.52
Ce700	84.5	5.410	23.12

The XRD analysis results of the CeO_2 samples with varying temperatures can be seen in Figure 3. All samples show the same diffraction pattern, with peaks appearing at 2θ = 28.5° (111), 33.09° (200), 47.5° (220), 56.3° (311), 59.08° (222), 69.4° (400), 77.1° (331), 79.07° (420), 88.4° (422), and 95.3° (511). According to JCPDS No. 00-034-0394, these peaks are characteristic of CeO_2 with a fluorite cubic crystal lattice (FCC). The absence of other peaks indicates that the synthesis at all temperatures produced pure CeO_2. As the temperature increases, the diffractogram peaks tend to shift to the left (Table 1). The peak shift is caused by changes in the lattice parameters induced by the elevated calcination temperatures [37]. The Ce500 and Ce600 samples have relative intensities that match the data from JCPDS No. 00-034-0394, indicating that the crystal growth direction in these samples aligns with the JCPDS standard. The Ce700 sample exhibits an increased diffraction intensity in the (220) and (311) planes, indicating that crystal growth in the sample tends to be oriented toward these planes [38].

The FWHM values of the samples decrease with increasing calcination temperature, indicating improved crystallinity. Higher temperatures enhance atomic arrangement, increasing the number of crystalline regions [26]. This increase in crystallinity boosts X-ray diffraction intensity [39]. The crystallite size of CeO_2, calculated using the Scherrer equation, also increases with rising calcination temperature, as higher temperatures cause pore interconnections [26]. Using Bragg's law, the interplanar spacing (d) and lattice parameter (a) for the (111) plane in Ce500, Ce600, and Ce700 samples were 3.120, 3.120, and 3.124 Å, and 5.406, 5.406, and 5.410 Å, respectively.

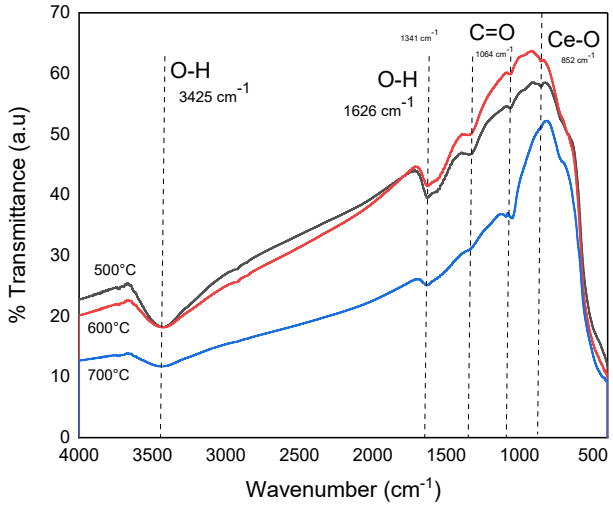

Figure 2. FTIR spectra of synthesized CeO_2

Table 3. The ratio of cerium atoms to oxygen atoms and CeO_2 particle size

Sample	% O atom	% Ce atom	Ce/O ratio	Particle size (µm)
Ce600	67.62	32.38	0.48	0.2-5.6
Ce700	63.70	36.30	0.57	0.12-2.9

SEM-EDS surface morphology analysis was conducted for Ce600 and Ce700 samples due to similar characterization results for Ce500 and Ce600 (Figures 4 and 5). The Ce700 sample shows more uniform and smaller particle sizes than Ce600. Using ImageJ, Ce600 particle sizes ranged from 0.2 to 5.6 µm, while Ce700 ranged from 0.12 to 2.9 µm. These findings contrast with Singh *et al.* [28], who reported increased particle size with higher calcination temperature. Ce and O element mapping show different surface profiles, with Ce700 having a more uneven surface than Ce600.

The EDS analysis results show that both samples have similar peaks. The distribution of Ce and O atoms on the surface of the CeO_2 samples can be seen in Table 2. In the Ce600 sample, the ratio of Ce/O atom counts is approximately 0.48, while in the Ce700 sample, it is 0.57. This indicates that in the Ce700 sample, more Ce atoms are exposed on the surface. This data is consistent with the SEM results, where Ce700 has smaller particle sizes. The decrease in the number of O atoms may also be related to the increase in catalytic sites caused by the increase in the number of oxygen vacancies on the surface [10].

The fluorescence properties of CeO_2 are shown in Figure 6. The sample was excited at λ = 247 nm and emitted light at λ = 496 nm, consistent with Windarti *et al.* [40]. The excitation spectrum of CeO_2 results from electrons moving from the 4f to the 5d orbital of Ce^{3+} ions. Instability in the 5d orbital causes electrons to return to the 4f orbital, emitting visible light [40]. The Ce600 sample has the highest excitation and emission intensity, likely due to fewer oxygen vacancies [41]. EDS results confirm that Ce600 has more O atoms than Ce700. The antioxidant and catalytic activity of CeO_2 increase with more oxygen vacancies and crystal defects [40], suggesting Ce700 has higher antioxidant activity than Ce500 and Ce600.

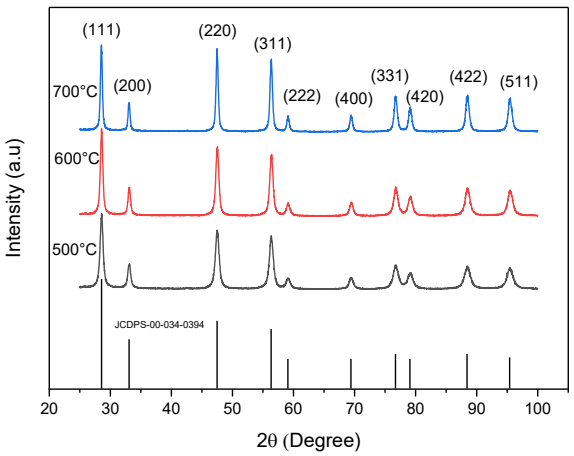

Figure 3. Diffractogram synthesized CeO_2

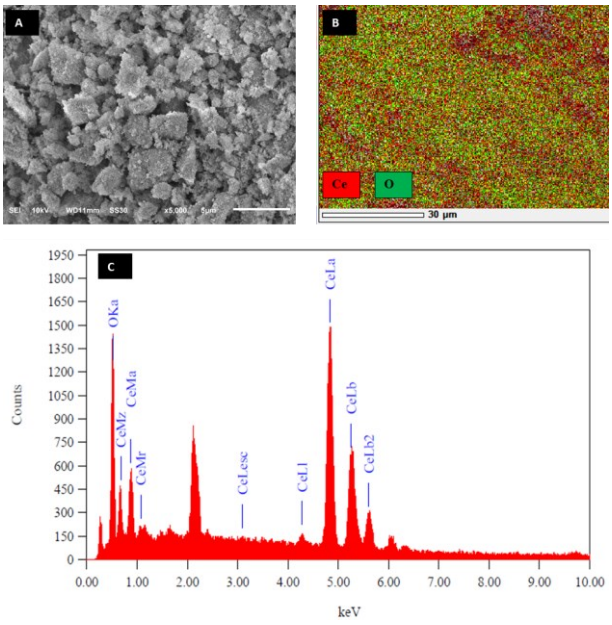

Figure 4. (A) SEM image, (B) SEM mapping, (C) EDS of CeO_2 calcinated at 600°C

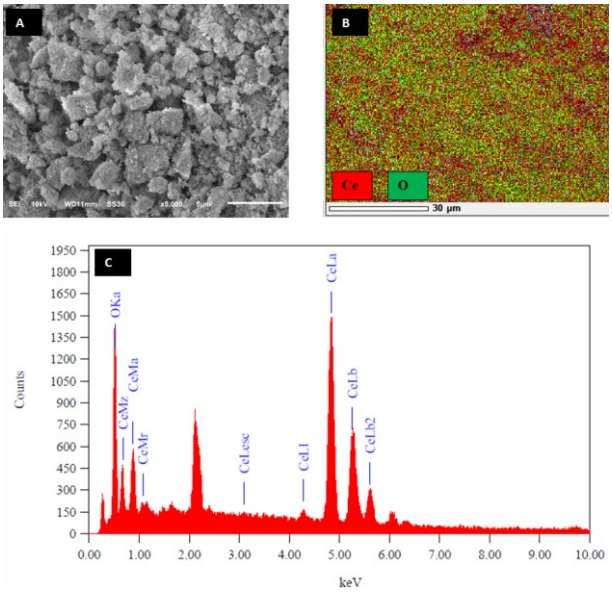

Figure 5. (A) SEM image, (B) SEM mapping, (C) EDS of CeO_2 calcinated at 700°C

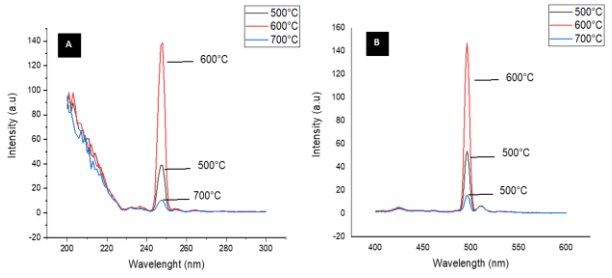

Figure 6. Fluorescence excitation and emission spectrum of synthesized CeO_2

4. Conclusion

Pure cerium oxide can be synthesized using the precipitation method at calcination temperatures of 500-700°C. The calcination temperature affects the characteristics of the resulting CeO_2, such as crystallinity, crystallite size, crystal parameters, surface morphology, and fluorescence properties. The crystallinity, crystallite size, and crystal parameter (a) of CeO_2 increase with the rising calcination temperature. Surface morphology shows that the shape of CeO_2 particles is irregular, with the size decreasing as the calcination temperature increases. The Ce/O ratio on the surface increases with higher calcination temperatures, indicating that cerium becomes more exposed on the surface. The fluorescence emission intensity does not correlate with the calcination temperature, with calcination at 600°C showing the highest fluorescence emission intensity (λ = 496 nm). Therefore, the selection of calcination temperature should be adjusted according to the intended application of CeO_2.

References

[1] Anna Shelyug, Alexandra Navrotsky, Thermodynamic stability of the fluorite phase in the CeO_2 - CaO - ZrO_2 system, *Journal of Nuclear Materials*, 517, (2019), 80-85 https://doi.org/10.1016/j.jnucmat.2019.01.043

[2] Ivana Celardo, Jens Z. Pedersen, Enrico Traversa, Lina Ghibelli, Pharmacological potential of cerium oxide nanoparticles, *Nanoscale*, 3, 4, (2011), 1411-1420 https://doi.org/10.1039/C0NR00875C

[3] Soichi Takasugi, Yugo Miseki, Kotaro Sasaki, Etsuko Fujita, Kazuhiro Sayama, Significance of an anion effect in the selective oxidation of Ce^{3+} to Ce^{4+} over a porous WO_3 photoanode, *Electrochimica Acta*, 307, (2019), 369-374 https://doi.org/10.1016/j.electacta.2019.03.178

[4] K. Kowsuki, R. Nirmala, Yong-Ho Ra, R. Navamathavan, Recent advances in cerium oxide-based nanocomposites in synthesis, characterization, and energy storage applications: A comprehensive review, *Results in Chemistry*, 5, (2023), 100877 https://doi.org/10.1016/j.rechem.2023.100877

[5] Ziwen Wang, Kaimeng Zhao, Shixiang Lu, Wenguo Xu, Application of flammulina-velutipes-like CeO_2/Co_3O_4/rGO in high-performance asymmetric supercapacitors, *Electrochimica Acta*, 353, (2020), 136599 https://doi.org/10.1016/j.electacta.2020.136599

[6] Andrea Cárdenas-Arenas, Helena Soriano Cortés, Esther Bailón-García, Arantxa Davó-Quiñonero, Dolores Lozano-Castelló, Agustín Bueno-López, Active, selective and stable NiO-CeO_2 nanoparticles for CO_2 methanation, *Fuel Processing Technology*, 212, (2021), 106637 https://doi.org/10.1016/j.fuproc.2020.106637

[7] Jaganathan Sakthi Yazhini Preetha, Duraisampath Sriram, Paramasivam Premasudha, Ramesh Namdeo Pudake, Muthukrishnan Arun, Cerium oxide as a nanozyme for plant abiotic stress tolerance: An overview of the mechanisms, *Plant Nano Biology*, 6, (2023), 100049 https://doi.org/10.1016/j.plana.2023.100049

[8] Alexander Filippi, Fobang Liu, Jake Wilson, Steven Lelieveld, Karsten Korschelt, Ting Wang, Yueshe Wang, Tobias Reich, Ulrich Pöschl, Wolfgang Tremel, Haijie Tong, Antioxidant activity of cerium dioxide nanoparticles and nanorods in scavenging hydroxyl radicals, *RSC Advances*, 9, 20, (2019), 11077-11081 https://doi.org/10.1039/C9RA00642G

[9] I. Nurhasanah, W. Safitri, Z. Arifin, A. Subagio, T. Windarti, Antioxidant activity and dose enhancement factor of CeO_2 nanoparticles synthesized by precipitation method, *IOP Conference Series: Materials Science and Engineering*, 432, (2018), 012031 https://doi.org/10.1088/1757-899X/432/1/012031

[10] Xiaojiao Yang, Ying Liu, Jun Li, Yuliang Zhang, Effects of calcination temperature on morphology and structure of CeO_2 nanofibers and their photocatalytic activity, *Materials Letters*, 241, (2019), 76-79 https://doi.org/10.1016/j.matlet.2019.01.006

[11] A. Balamurugan, M. Sudha, S. Surendhiran, R. Anandarasu, S. Ravikumar, Y. A. Syed Khadar, Hydrothermal synthesis of samarium (Sm) doped cerium oxide (CeO_2) nanoparticles: Characterization and antibacterial activity, *Materials Today: Proceedings*, 26, (2020), 3588-3594 https://doi.org/10.1016/j.matpr.2019.08.217

[12] N. S. Ferreira, R. S. Angélica, V. B. Marques, C. C. O. de Lima, M. S. Silva, Cassava-starch-assisted sol–gel synthesis of CeO_2 nanoparticles, *Materials Letters*, 165, (2016), 139-142 https://doi.org/10.1016/j.matlet.2015.11.107

[13] Yoki Yulizar, Sumandi Juliyanto, Sudirman, Dewangga Oky Bagus Apriandanu, Rizki Marcony Surya, Novel sol-gel synthesis of CeO_2 nanoparticles using *Morinda citrifolia* L. fruit extracts: Structural and optical analysis, *Journal of Molecular Structure*, 1231, (2021), 129904 https://doi.org/10.1016/j.molstruc.2021.129904

[14] Mmajid Farahmandjou, Mahkameh Dastpak, Synthesis of Fe-doped CeO_2 Nanoparticles Prepared by Solgel Method, *Journal of Sciences, Islamic Republic of Iran*, 31, 1, (2020), 39-43 https://doi.org/10.22059/jsciences.2020.256813.1007255

[15] Natarajan Sisubalan, Vijayan Sri Ramkumar, Arivalagan Pugazhendhi, Chandrasekaran Karthikeyan, Karuppusamy Indira, Kasi Gopinath, Abdulrahman Syedahamed Haja Hameed, Mohamed Hussain Ghouse Basha, ROS-mediated cytotoxic activity of ZnO and CeO_2 nanoparticles synthesized using the *Rubia cordifolia* L. leaf extract on MG-63 human osteosarcoma cell lines, *Environmental Science and Pollution Research*, 25, 11, (2018), 10482-10492 https://doi.org/10.1007/s11356-017-0003-5

[16] Saynaz Aseyd Nezhad, Ali Es-haghi, Masoud Homayouni Tabrizi, Green synthesis of cerium oxide nanoparticle using *Origanum majorana* L. leaf extract, its characterization and biological activities, *Applied Organometallic Chemistry*, 34, 2, (2020), e5314 https://doi.org/10.1002/aoc.5314

[17] Asghar Zamani, Ahmad Poursattar Marjani, Khadijeh Alimoradlu, Walnut Shell-Templated Ceria Nanoparticles: Green Synthesis, Characterization and Catalytic Application, *International Journal of Nanoscience*, 17, 06, (2018), 1850008 https://doi.org/10.1142/S0219581X18500084

[18] J. Malleshappa, H. Nagabhushana, B. Daruka Prasad, S. C. Sharma, Y. S. Vidya, K. S. Anantharaju, Structural, photoluminescence and thermoluminescence properties of CeO_2 nanoparticles, *Optik*, 127, 2, (2016), 855-861 https://doi.org/10.1016/j.ijleo.2015.10.114

[19] Sanjivani V. Umale, Sneha N. Tambat, Sharad M. Sontakke, Combustion synthesized CeO_2 as an anodic material in dye sensitized solar cells, *Materials Research Bulletin*, 94, (2017), 483-488 https://doi.org/10.1016/j.materresbull.2017.07.004

[20] Balaraju Bayyappagari, Kaleemulla Shaik, Madhusudhana Rao Nasina, Omkaram Inturu, Sreekantha Reddy Dugasani, Effect of Fe substitution on optical and magnetic properties of CeO_2 nanoparticles, *Optik*, 154, (2018), 821-827 https://doi.org/10.1016/j.ijleo.2017.10.025

[21] Sumetha Suwanboon, Pongsaton Amornpitoksuk, Phuwadol Bangrak, The improvement of the band gap energy and antibacterial activities of CeO_2/ZnO nanocomposites prepared by high energy ball milling, *Warasan Khana Witthayasat Maha Witthayalai Chiang Mai*, 45, (2018), 1129-1137

[22] Huey-Ing Chen, Hung-Yi Chang, Synthesis of nanocrystalline cerium oxide particles by the precipitation method, *Ceramics International*, 31, 6, (2005), 795-802 https://doi.org/10.1016/j.ceramint.2004.09.006

[23] M. Farahmandjou, M. Zarinkamar, T. P. Firoozabadi, Synthesis of Cerium Oxide (CeO_2) nanoparticles using simple CO-precipitation method, *Revista mexicana de física*, 62, (2016), 496-499

[24] M. Ramachandran, R. Subadevi, M. Sivakumar, Role of pH on synthesis and characterization of cerium oxide (CeO_2) nano particles by modified co-precipitation method, *Vacuum*, 161, (2019), 220-224 https://doi.org/10.1016/j.vacuum.2018.12.002

[25] M. Li, R. Zhang, H. Zhang, W. Feng, X. Liu, Synthesis, structural and magnetic properties of CeO_2 nanoparticles, *Micro & Nano Letters*, 5, 2, (2010), 95-99 https://doi.org/10.1049/mnl.2009.0092

[26] Iis Nurhasanah, Weni Safitri, Tri Windarti, Agus Subagio, The Calcination Temperature Effect on The Antioxidant and Radioprotection Properties of CeO_2 Nanoparticles, *Reaktor*, 18, 1, (2018), 22-26 https://doi.org/10.14710/reaktor.18.1.22-26

[27] Yuliia Shlapa, Serhii Solopan, Veronika Sarnatskaya, Katarina Siposova, Ivana Garcarova, Katerina Veltruska, Illia Timashkov, Oleksandra Lykhova, Denis Kolesnik, Andrey Musatov, Vladimir Nikolaev, Anatolii Belous, Cerium dioxide nanoparticles synthesized via precipitation at constant pH: Synthesis, physical-chemical and antioxidant properties, *Colloids and Surfaces B: Biointerfaces*, 220, (2022), 112960 https://doi.org/10.1016/j.colsurfb.2022.112960

[28] Rahul Dheerendra Singh, Prashant Bhimrao Koli, Bapu Sonu Jagdale, Arun Vitthal Patil, Effect of firing temperature on structural and electrical parameters of synthesized CeO_2 thick films, *SN Applied Sciences*, 1, 4, (2019), 315 https://doi.org/10.1007/s42452-019-0246-5

[29] Kota Shiba, Satoshi Motozuka, Tadashi Yamaguchi, Nobuhiro Ogawa, Yuichi Otsuka, Kiyoshi Ohnuma, Takuya Kataoka, Motohiro Tagaya, Effect of Cationic Surfactant Micelles on Hydroxyapatite Nanocrystal Formation: An Investigation into the Inorganic–Organic Interfacial Interactions, *Crystal Growth & Design*, 16, 3, (2016), 1463-1471 https://doi.org/10.1021/acs.cgd.5b01599

[30] Ata Chitsaz, Marzieh Jalilpour, Mohammad Fathalilou, Effects of PVP and CTAB surfactants on the morphology of cerium oxide nanoparticles synthesized via co-precipitation method, *International Journal of Materials Research*, 104, 5, (2013), 511-514 https://doi.org/10.3139/146.110927

[31] R. Suresh, V. Ponnuswamy, R. Mariappan, Effect of annealing temperature on the microstructural, optical and electrical properties of CeO_2 nanoparticles by chemical precipitation method, *Applied Surface Science*, 273, (2013), 457-464 https://doi.org/10.1016/j.apsusc.2013.02.062

[32] V. Morris, P. G. Fleming, J. D. Holmes, M. A. Morris, Comparison of the preparation of cerium oxide nanocrystallites by forward (base to acid) and reverse (acid to base) precipitation, *Chemical Engineering Science*, 91, (2013), 102-110 https://doi.org/10.1016/j.ces.2013.01.016

[33] S. A. Hassanzadeh-Tabrizi, Mehdi Mazaheri, M. Aminzare, S. K. Sadrnezhaad, Reverse precipitation synthesis and characterization of CeO_2 nanopowder, *Journal of Alloys and Compounds*, 491, 1, (2010), 499-502 https://doi.org/10.1016/j.jallcom.2009.10.243

[34] G. Jayakumar, A. Albert Irudayaraj, A. Dhayal Raj, Investigation on the synthesis and photocatalytic activity of activated carbon–cerium oxide (AC–CeO_2) nanocomposite, *Applied Physics A*, 125, 11, (2019), 742 https://doi.org/10.1007/s00339-019-3044-4

[35] Georgi N. Vayssilov, Mihail Mihaylov, Petko St Petkov, Konstantin I. Hadjiivanov, Konstantin M. Neyman, Reassignment of the Vibrational Spectra of Carbonates, Formates, and Related Surface Species on Ceria: A Combined Density Functional and Infrared Spectroscopy Investigation, *The Journal of Physical Chemistry C*, 115, 47, (2011), 23435-23454 https://doi.org/10.1021/jp208050a

[36] P. A. Sheena, K. P. Priyanka, Boby Sabu, Thomas Varghese, Effect of calcination temperature on the structural and optical properties of nickel oxide nanoparticles, *Nanosystems: Physics, Chemistry, Mathematics*, 5, 3, (2014), 441-449

[37] H. F. Lopez, H. Mendoza, Temperature Effects on the Crystallization and Coarsening of Nano-CeO_2 Powders, *ISRN Nanomaterials*, 2013, (2013), 208614 https://doi.org/10.1155/2013/208614

[38] Yuki Tsuda, Kyota Uda, Misaki Chiba, He Sun, Lina Sun, Matthew Schuette White, Akito Masuhara, Tsukasa Yoshida, Selective hybridization of organic dyes with CuSCN during its electrochemical growth, *Microsystem Technologies*, 24, 1, (2018), 715-723 https://doi.org/10.1007/s00542-017-3394-9

[39] Mario E Rodriguez-Garcia, Sandra M Londoño-Restrepo, Cristian F Ramirez-Gutierrez, Beatriz Millan-Malo, Effect of the crystal size on the X-ray diffraction patterns of isolated orthorhombic starches: A-type, *arXiv preprint arXiv*, (2018), 1808.02966 https://doi.org/10.48550/arXiv.1808.02966

[40] Tri Windarti, Anita Listiyani Dewi, Cahaya Ratu Indra Bulan, Regita Pramesti, Sintesis CeO_2 Dengan Metode Green Synthesis: Studi Sifat Fluoresen, *Greensphere: Journal of Environmental Chemistry*, 2, 2, (2023), 13-17

[41] Biswajit Choudhury, Pawan Chetri, Amarjyoti Choudhury, Annealing temperature and oxygen-vacancy-dependent variation of lattice strain, band gap and luminescence properties of CeO_2 nanoparticles, *Journal of Experimental Nanoscience*, 10, 2, (2015), 103-114 https://doi.org/10.1080/17458080.2013.801566